Journal of South American Earth Sciences 72 (2016) 227–240

Contents lists available at ScienceDirect

Journal of South American Earth Sciences

journal homepage: www.elsevier.com/locate/jsames

High-pressure/low-temperature metamorphism in the collision zone between the Chilenia and Cuyania microcontinents (western Precordillera, Argentina)

F.L. Boedo [a, *], A.P. Willner [b, c], G.I. Vujovich [a], H.-J. Massonne [b]

[a] Instituto de Estudios Andinos "Don Pablo Groeber" (UBA-CONICET), Int. Güiraldes 2160 (1428), Departamento de Ciencias Geológicas, Facultad de Ciencias Exactas y Naturales, Universidad de Buenos Aires, Argentina
[b] Institut für Mineralogie und Kristallchemie, Universität Stuttgart, Azenbergstr. 18, 70174, Stuttgart, Germany
[c] Institut für Geologie, Mineralogie und Geophysik, Ruhr-Universität, 44780, Bochum, Germany

ARTICLE INFO

Article history:
Received 9 May 2016
Received in revised form
5 September 2016
Accepted 8 September 2016
Available online 9 September 2016

Keywords:
Peñasco formation
Mafic-ultramafic belt
Devonian
Greenschist facies
Geothermobarometry
Pseudosections
Phengite

ABSTRACT

In central-western Argentina, an Early Paleozoic belt including mafic-ultramafic bodies, marine metasedimentary rocks and high-pressure rocks occur along the western margin of the Precordillera and in the Frontal Cordillera. First pressure-temperature estimates are presented here for low-grade rocks of the southern sector of this belt based on two metasedimentary and one metabasaltic sample from the Peñasco Formation. Peak metamorphic conditions resulted within the range of 345–395 °C and 7.0–9.3 kbar within the high-pressure greenschist facies. The corresponding low metamorphic gradient of 13 °C/km is comparable with subduction related geothermal gradients. Comparison between these results and data from other localities of the same collision zone (Guarguaraz and Colohuincul complexes) confirms a collision between Chilenia and the composite margin of western Gondwana and suggests a stronger crustal thickening in the south of the belt, causing exhumation of more deeply buried sequences. During the Early Paleozoic a long-lived marine sedimentation coupled with the intrusion of MORB-like basalts occurred along a stable margin before the collision event. This contrasts with the almost contemporaneous sedimentation registered during accretion in accretionary prism settings and additionally proves the development of a collision zone along western Precordillera and the eastern Frontal Cordillera as well as the existence of Chilenia as a separate microcontinent.

1. Introduction

During Early Paleozoic times, several microcontinents (e.g. Paracas, Cuyania, Chilenia and others) collided with the western margin of Western Gondwana (current South American Plate; e.g. Ramos, 2009). The recognition of their respective sutures was originally mainly based on the presence of mafic-ultramafic belts or regional lineaments along such hypothesized boundaries. Particularly, in central-western Argentina a linear chain of several mafic and ultramafic bodies occurs over 400 km which was first interpreted as a suture zone between the composite western Gondwana margin (after Ordovician collision of the Cuyania microcontinent) and the Chilenia microcontinent by Haller and Ramos (1984) and Ramos *et al.* (1986).

There is still a debate on numerous aspects of the collision event mostly regarding the provenance of the Chilenia terrane (if it is allochthonous or parautochthonous to Gondwana). Do the mafic-ultramafic bodies belong to different geotectonic environments or belong they to the same ancient oceanic lithosphere section? Which was the subduction polarity of the Chilenia terrane when it approached to the Gondwana margin? Where was the corresponding magmatic arc located?

The presence of the mafic-ultramafic belt is so far one of the main evidences that support the existence of Chilenia as a separate microcontinent. Late Neoproterozoic to Early Paleozoic metasedimentary rocks associated to mafic and ultramafic bodies from the Precordillera and the Frontal Cordillera exhibit similar structural styles and polyphase deformation; intense isoclinal and disharmonic folding, crenulation cleavage and double-vergent

* Corresponding author.
E-mail addresses: florenciaboedo@gmail.com (F.L. Boedo), arne.willner@rub.de (A.P. Willner), graciela@gl.fcen.uba.ar (G.I. Vujovich), h-j.massonne@imi.uni-stuttgart.de (H.-J. Massonne).

http://dx.doi.org/10.1016/j.jsames.2016.09.009
0895-9811/

deformation (von Gosen, 1997; Davis *et al.*, 1999; Gerbi *et al.*, 2002; López, 2005; Giambiagi *et al.*, 2010). Studies on metamorphism of metabasites and metasedimentary rocks along the belt and further south have provided critical evidence for collision processes (Davis *et al.*, 1999; Robinson *et al.*, 2005; Massonne and Calderón, 2008; Willner *et al.*, 2008, 2011; Gargiulo *et al.*, 2011, 2012, 2013, Boedo *et al.*, 2012, this work).

The purpose of this contribution is to characterize the pressure-temperature (P-T) metamorphic conditions of the metasedimentary and metabasaltic rocks from the Peñasco area, part of the southern sector of the Precordillera mafic-ultramafic belt. Furthermore, we correlate our new P-T data with those obtained from the southernmost sector of the mafic-ultramafic belt (Guarguaraz Complex; Massonne and Calderón, 2008; Willner *et al.*, 2011) and the extension of the corresponding collisional suture to the Colohuincul Complex (Martínez *et al.*, 2012).

2. Geological setting

2.1. The Argentine Precordillera

The Argentine Precordillera is a fold and thrust belt which is located in central-western Argentina and developed along the western margin of the Cuyania composite terrane (Fig. 1a). Its Early Paleozoic stratigraphy is well documented with dominating sequences of platform limestones to the east and marine siliciclastic sedimentary rocks to the west, where mafic-ultramafic bodies, affected by very low to low-grade metamorphism (e.g. Davis *et al.*, 1999; Rubinstein *et al.*, 2000; Robinson *et al.*, 2005; Boedo *et al.*, 2012, 2015), are intercalated (Haller and Ramos, 1984; Astini *et al.*, 1995; Thomas and Astini, 2003).

The western Argentine Precordillera consists of metasedimentary rocks which originated in deep marine and continental slope settings, including platform carbonate and siliciclastic olistoliths from its basement (Thomas and Astini, 2003 and references therein). These rocks are spatially related to mafic-ultramafic bodies within the Precordillera mafic-ultramafic belt. The outcrops of this belt are discontinuous between latitudes 28° and 33°S and consist of serpentinized ultramafic rocks, mafic granulites, together with massive metagabbros, metabasaltic dikes, sills and pillow lavas. The mafic rocks have N- to E-MORB (Normal-to Enriched-Mid-Ocean Ridge Basalts) signature and positive ε_{Nd} values (+6 to +9.3), which are compatible with basalts/gabbros from the oceanic crust (Haller and Ramos, 1984; Kay *et al.*, 1984; Cortés and Kay, 1994; Fauqué and Villar, 2003; González Menéndez *et al.*, 2013; Boedo *et al.*, 2013). The vergence of deformation in Early Paleozoic units is still a matter of debate. Most authors postulate that it is to the west based on the main vergence of major structures (Ramos *et al.*, 1986; von Gosen, 1997; Cortés *et al.*, 1999; Ariza *et al.*, 2015), whereas others propose an eastward vergence on the basis of only localized kinematic indicators within allochtonous granulite lenses (Davis *et al.*, 1999; Gerbi *et al.*, 2002; Álvarez Marrón *et al.*, 2006), which may have been rotated as they show different orientations along strike regarding the main foliation (S_1) in metasedimentary rocks (Boedo, 2015).

The Precordillera mafic-ultramafic belt can be divided in two sectors according to their rock association and metamorphic grade: a northern sector, which comprises the outcrop localities of Jagüé, Rodeo, Tigre and Calingasta, and a southern sector with the outcrop areas of Peñasco, Pozos, Cerro Redondo, Cortaderas and Bonilla (Fig. 1a). A very low to low-grade metamorphic imprint is registered along the northern part of the belt (Cucchi, 1971; Buggisch *et al.*, 1994; Robinson *et al.*, 2005), while a low to medium grade metamorphic imprint affects its southern part, where intercalations of retrograded mafic granulite (a former layered gabbro complex) also occur (Davis *et al.*, 1999; Boedo *et al.*, 2012). Haller and Ramos (1984) assumed that the southernmost part of the mafic-ultramafic belt is located in the Sierra de Guarguaraz within the Frontal Cordillera (Fig. 1b), where serpentinite, metagabbro, metabasaltic dikes and pillow lavas occur in contact with marble and schist of sedimentary origin (Villar, 1969, 1970; Gregori and Bjerg, 1997; López de Azarevich *et al.*, 2009; Gargiulo *et al.*, 2011). These lithological units are grouped in the Guarguaraz Complex (López and Gregori, 2004). Despite their particular differences, the mafic and ultramafic bodies from the Precordillera and Frontal Cordillera are considered to belong to a dismembered ophiolite along the suture zone between the composite western Gondwana margin (after Ordovician collision of the Cuyania microcontinent) and the Chilenia microcontinent (Fig. 1a–b) (Haller and Ramos, 1984; Ramos *et al.*, 1986).

U/Pb ages on detrital zircon show a maximum age of deposition of 555 ± 8 Ma for the (meta)sediments of the Guarguaraz Complex (Willner *et al.*, 2008), which is consistent with findings of cyanobacteria and acritarchs of probable Vendian-Cambrian age and an age of 655 ± 76 Ma (Sm-Nd whole-rock) for an intercalated metabasite (López de Azarevich *et al.*, 2009), interpreted by them as the probable crystallization age of the protolith. Similar to the western Precordillera, the mafic bodies have N- to E-MORB chemical signature and the whole sequence is strongly deformed and metamorphosed. Massonne and Calderón (2008) estimated an early P-T stage of 8 kbar, 470–500 °C in metapelites and a subsequent pressure increase (13.5 kbar, 500 °C) followed by a decompression to 8 kbar, 565 °C. Willner *et al.* (2011) determined similar high pressure conditions (12–14 kbar, 470–530 °C) in metabasite and metapelite, followed by a decompression with a slight increase in temperature (5 kbar, 560 °C).

Regarding P-T conditions in the northern part of the Precordillera, Rubinstein *et al.* (1998, 2000) and Robinson *et al.* (2005) estimated very low to low-grade and low pressure conditions (2–3 kbar, 250-350 °C) in metabasite and metapelite from the Alcaparrosa and Yerba Loca formations in the Calingasta and Rodeo areas, respectively. P-T estimates by Davis *et al.* (1999) for the Cortaderas mafic granulites in the southern part of the Precordillera yielded temperatures between 850 and 1000 °C at 11 kbar. Boedo *et al.* (2012) estimated similar conditions in mafic granulite from the Cordón del Peñasco area (P > 9 kbar, T~885 °C).

To the south, in the North Patagonian Andes, rocks from the Colohuincul Complex (Fig. 1a) exhibit metamorphic trajectories deduced to be the result of thermal relaxation after crustal thickening (Martínez *et al.*, 2012). These authors also interpret these processes as a consequence of the Chilenia collision against the western Gondwana margin and extend the microcontinent up to the 41°S (present coordinates).

Dating of the metamorphic event in low and medium grade rocks from the Precordillera, Frontal Cordillera and North Patagonian Andes generally yielded Devonian ages (Cucchi, 1971; Buggisch *et al.*, 1994; Davis *et al.*, 1999; Willner *et al.*, 2011; Martínez *et al.*, 2012).

The mafic-ultramafic belt, which is considered as an almost complete ophiolite sequence, represents oceanic crust that may have been subducted shortly before the collision of the Chilenia microcontinent with the western Gondwana margin in the Middle Devonian (Haller and Ramos, 1984; Ramos *et al.*, 1986; Willner *et al.*, 2011). However, Davis *et al.* (2000) proposed that the mafic granulite in the Precordillera could partly represent the roots of a magmatic arc.

After exhumation of the Chilenia collision zone, marine sediments of Early Carboniferous age unconformably overlie all basement rocks (Amos and Rolleri, 1965).

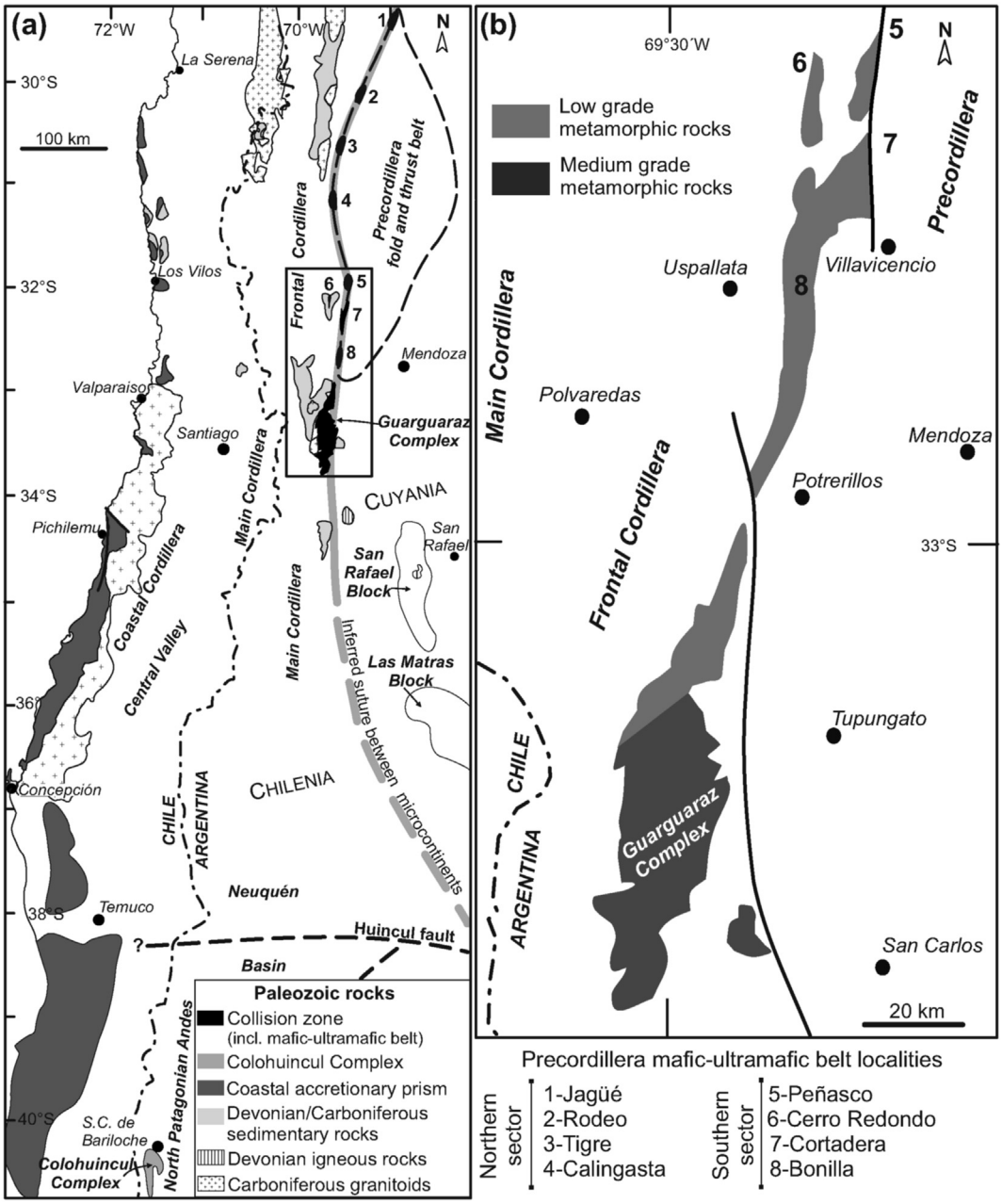

Fig. 1. a) Schematic map from central-western Argentina and central Chile. The light grey line marks the suture zone between the Chilenia and Cuyania microcontinents. The black square indicates the location of the map in Fig. 1b. **b)** Simplified regional map from the southern sector of the Precordillera mafic-ultramafic belt and eastern Frontal Cordillera (Guarguaraz Complex). Map modified from Caminos (1993).

2.2. The Cordón del Peñasco area

Our study zone is located in the Cordón del Peñasco, in the northern province of Mendoza (Fig. 2). A wide variety of nomenclature schemes have been proposed for the Early Paleozoic rocks exposed in this area and current stratigraphic nomenclature is invalid (Boedo, 2015). Therefore, we propose the term Cortadera Complex to designate the lithological units originally described by Harrington (1971) as "facies Cortadera". This unit comprises lenses of serpentinite (harzburgite, dunite, wehrlite, lherzolite) and retrograded mafic granulite (former layered gabbro) in tectonic contact with phyllite and subordinated metacarbonate. Occasionally, serpentinite and metasedimentary rocks are intruded by E-MORB (meta)basaltic dikes. Because all contacts are tectonic and due to strong internal deformation, the unit thickness is unknown (Harrington, 1971). The Cortadera Complex is assigned to the Neoproterozoic-Cambrian? on the basis of stratigraphic relations and an age of 576 ± 17 Ma (U/Pb on zircon) obtained on a metabasaltic dike (Davis *et al.*, 2000).

The Cortadera Complex is in tectonic contact with the Peñasco Formation (Fig. 2). Our work adopts the criteria employed by Cortés *et al.* (1999) who defined the Peñasco Formation as the siliciclastic metasedimentary succession present in the study area, which is equivalent to the "facies Normal" early described by Harrington (1971). This unit comprises up to 2 m thick layers of medium to fine-grained metagreywacke alternating with metapelite. Scarce pelitic deposits crop out in some regions. Occasionally, amalgamated medium-grained metagreywacke, thick coarse-grained

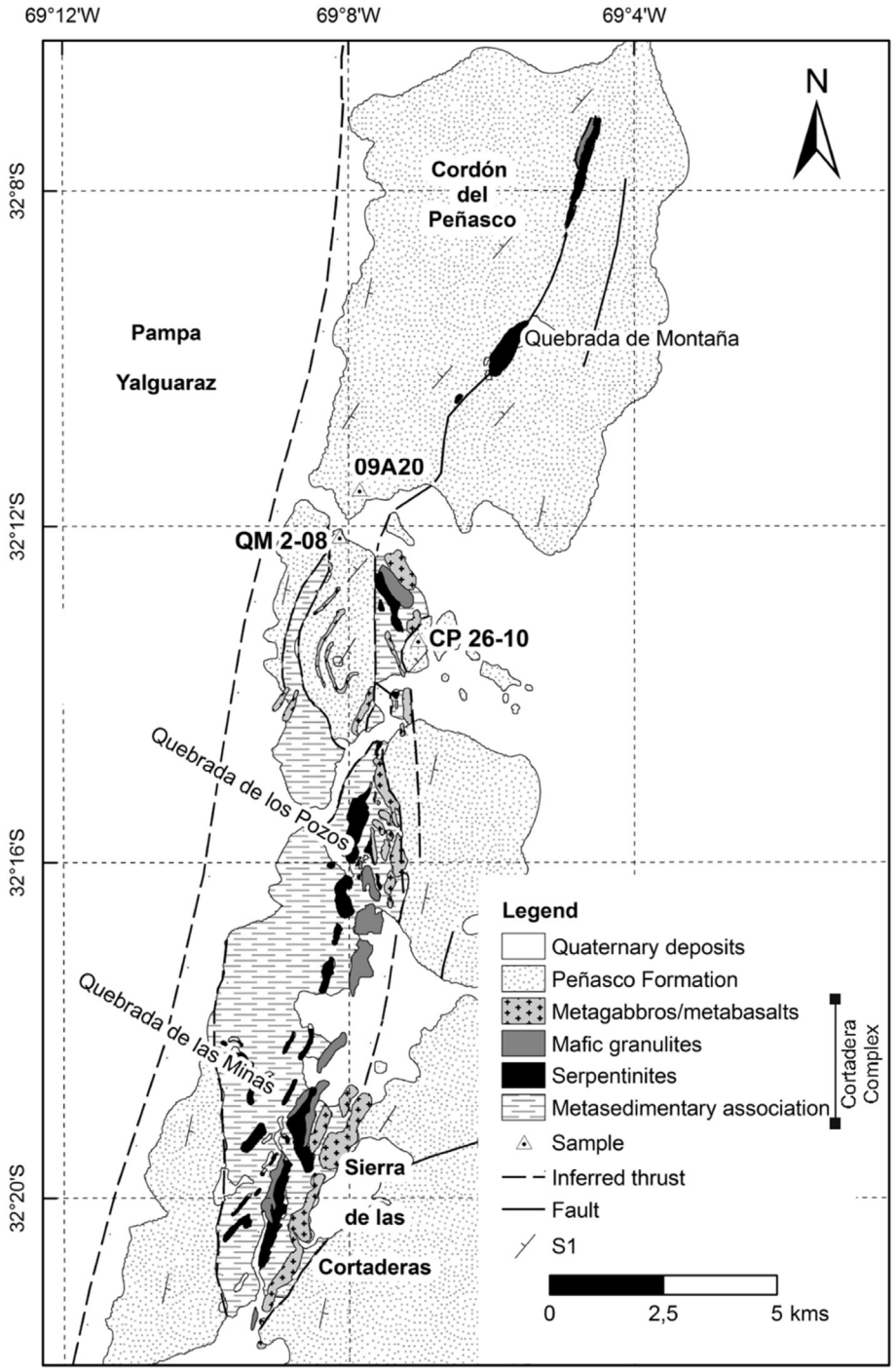

Fig. 2. Simplified geological map from the Peñasco-Cortaderas area after Davis *et al.* (1999) and Boedo (2015) with locations of the analyzed samples indicated by triangles.

metagreywacke and fine-grained metaconglomerate occur. To the east of the study area, fining-upwards cycles and sedimentary structures such as flute marks, inverse grading, load casts, horizontal lamination and ripples were observed (Boedo *et al.*, 2012; Boedo, 2015). The succession is intruded by E-MORB (meta) basaltic dikes and sills. To the west, metavolcanic rocks, metabasalt and metahyaloclastite are more frequently intercalated. The preserved strata and sedimentary structures indicate a turbiditic sedimentation in proximal areas and associated metabasaltic dikes and sills and metahyaloclastite suggest a shallow oceanic basin to the west of the Cuyania microcontinent (Boedo *et al.*, 2013).

The Peñasco Formation is assigned to the Ordovician-Early Devonian on the basis of stratigraphic relations (Cortés *et al.*, 1999). The metasedimentary rocks show three main foliations: S_0 (bedding), S_1 (main foliation) and S_2 (crenulation cleavage) (Fig. 3a–b). Metamorphic grade and deformation increase from east to west. To the east, S_1 affects only fine-grained rock types with little or no mineral recrystallization, whereas to the west, S_1 is well developed (in many cases, S_0 coincides with S_1) and S_2 may appear.

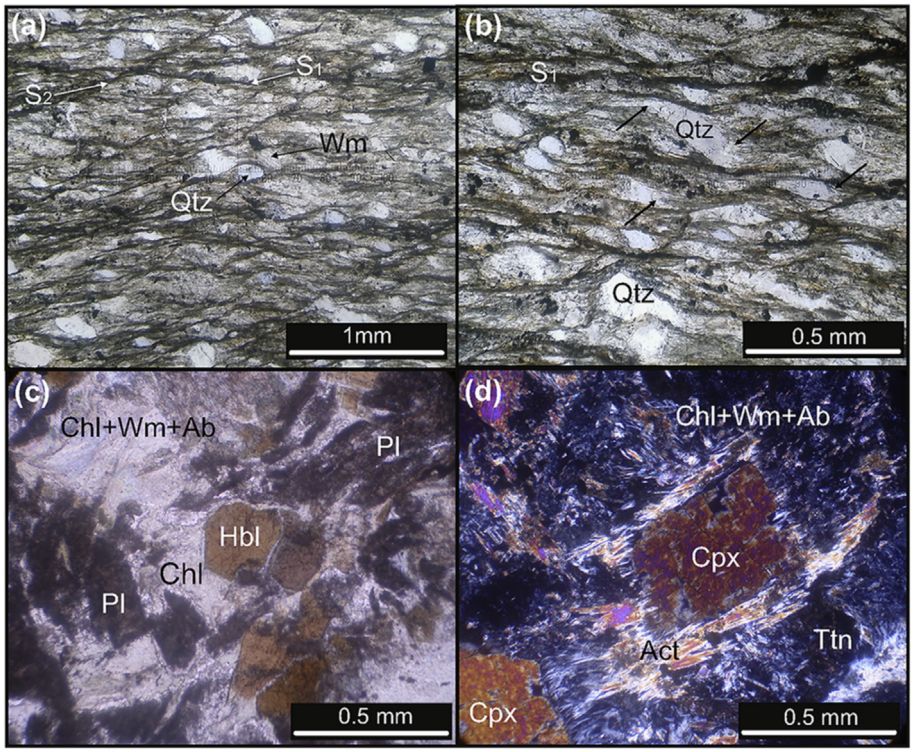

Fig. 3. Thin-section photomicrographs. **a)** Plane-polarized light. Sample CP 26-10 showing spaced foliation (S_1) and incipient crenulation cleavage (S_2). Microlithons are composed of quartz (Qtz) and minor plagioclase and detrital mica (Wm), whereas cleavage domains consist of oriented chlorite, white mica and opaque minerals. **b)** Plane-polarized light. Sample CP 26–10 exhibiting spaced foliation (S_1) where detrital quartz (Qtz) shows pressure-dissolution effects (black arrows). **c)** Plane-polarized light. Metabasalt QM 2–08 with saussuritized plagioclase (Pl) and brownish amphibole (Hbl) in a matrix composed of chlorite (Chl), white mica (Wm) and albite (Ab). **d)** Crossed-polarized light. Relic of clinopyroxene (Cpx) surrounded by fibrous actinolite (Act). Titanite (Ttn) is also present and partially replaces original ilmenite crystals. (For interpretation of the references to colour in this figure legend, the reader is referred to the web version of this article.)

3. Materials and methods

3.1. Sample preparation and analyses

Representative rock types from the Peñasco area were sampled (Fig. 2). Based on thin-section studies, we selected three samples containing white mica: one mafic sample (QM2-08) and two metasedimentary samples (09A20 and CP 26–10), in order to perform the petrological investigation documented in our contribution.

Samples were prepared and analyzed following standard procedures. Special efforts were made to avoid samples containing veins. The whole-rock major and trace element concentrations were analyzed at ACTLABS Laboratories (Canada) following the lithium metaborate/tetraborate fusion procedure and subsequent ICP-MS analytics. The compositions of mineral phases were analyzed with a CAMECA SX100 electron microprobe at Institut für Mineralogie und Kristallchemie, Universität Stuttgart, Germany. Operating conditions on the routine mineral analyses were a beam current of 15 kV, a beam diameter of about 5 μm and acceleration voltage of 10 nA. Counting time per element were 20 s at the peak and on the background. Standards were natural minerals (e.g. wollastonite for Si and Ca Kα1, rutile for TiKα1, rhodonite for MnKα1), pure oxides (e.g. Fe_2O_3 for FeKα1) and glass (e.g. Ba glass for BaLα1). The PAP correction procedure provided by CAMECA was applied.

The proportion of cations for white mica is based on 42 negative charges neglecting the interlayer cations; the sum of octahedrally coordinated cations is set at 4·1 to allow for an estimation of Fe^{3+}. For chlorite, cations are based on 56 negative charges; H_2O is calculated on the basis of the structural formula with OH = 16.

3.2. Geothermobarometric methods

Based on bulk-rock composition of the samples, the minimum Gibbs energy relation was calculated with the computer program PERPLE_X (Connolly, 1990; version 6.6) to construct P-T pseudosections in the system Si-Ti-Al-Ca-Fe-Mg-K-Na-O-H. This chemical system was applied for both mafic and metasedimentary samples. Bulk-rock compositions were simplified to the above 10-component system by (1) adding MnO to FeO, (2) removing P_2O_5 combined with a reduction of CaO considering that phosphorus is only bound to pure apatite, and (3) increasing H_2O to excess conditions considered to have prevailed during metamorphism. O_2 contents were estimated to account for trivalent Fe in epidote and pumpellyite (Table 1). Subsequently, the bulk-rock compositions were normalized to 100% (Table 1).

Samples were modeled in the P-T range of 2–10 kbar and 200-400 °C with the PERPLE_X software. For this purpose, the internally consistent thermodynamic data set of Holland and Powell (1998, updated 2003) for minerals and aqueous fluid was applied, with the addition of end-member data for Fe^{2+}- and Fe^{3+}-pumpellyite, Fe^{2+}- and Mg-stilpnomelane, actinolite and magnesioriebeckite (Massonne and Willner, 2008). Calculations were performed using the solid-solution models of Powell and Holland (1999) and Holland and Powell (2003) for white mica, epidote, chlorite and biotite and those of Massonne and Willner (2008) for amphibole, sodic clinopyroxene, pumpellyite and stilpnomelane. The clinopyroxene model is that of Holland and Powell (1996) supplemented by the acmite component, which is commonly enhanced at very

Table 1
Bulk-rock compositions of the studied samples. Analyzed major element contents in metasedimentary rocks (09A20 and CP 26–10) and metabasalt (QM 2–08) compared with simplified and normalized values for the selected chemical system.

Composition (in wt.%)	CP 26–10 analyzed	CP 26-10 simplified and normalized	09A20 analyzed	09A20 simplified and normalized	QM 2–08 analyzed	QM 2–08 simplified and normalized
SiO_2	72.92	71.04	65.77	64.08	46.04	43.06
Al_2O_3	11.26	10.97	16.00	15.59	16.97	15.87
TiO_2	0.90	0.88	0.80	0.78	1.32	1.23
FeO	4.91	4.85	–	6.32	9.21	8.75
Fe_2O_3	0.36	–	7.04	–	1.01	–
MnO	0.07	–	0.14	–	0.15	–
MgO	1.55	1.51	2.14	2.08	7.13	6.67
CaO	0.96	0.72	0.35	0.18	12.55	11.58
Na_2O	2.19	2.13	1.64	1.60	2.03	1.90
K_2O	1.95	1.90	3.48	3.37	1.00	0.94
P_2O_5	0.17	–	0.13	–	0.12	–
O_2	–	0.00	–	0.00	–	0.40
H_2O	–	6.00	–	6.00	–	9.60
Total	97.24	100.00	97.47	100.00	97.53	100.00

low-grade conditions. Albite, K-feldspar, prehnite, quartz, titanite, H_2O, ilmenite and magnetite were considered as pure phases. Willner *et al.* (2013) showed that the pseudosection technique is particularly suitable to model very low to low-grade metamorphic rocks: (1) A maximum of fluid is usually present, (2) individual mineral grains are small and typically unzoned without overgrown cores, and (3) relict and prograde phases are interconnected by the fluids produced and are part of the reacting bulk-rock composition.

Maximum P-T conditions were estimated with the aid of P-T pseudosections by a combination of the P-T field of the observed assemblage in the studied samples and the isopleth of the maximum Si content observed in white mica. Although the Si isopleths of white mica can show different dP/dT slopes in pseudosections of metasedimentary and metabasalt samples, the Si content in white mica often increases with pressure. Therefore, it can be employed as a geothermobarometer (Willner *et al.*, 2013). The confidence on white mica is due to the strong variation of Si content in the selected P-T range and mostly (but not always) pressure-dependent.

4. Petrographic and mineral chemical features

Sample CP 26–10 is a fine to medium-grained metagreywacke with granoblastic texture and a pronounced spaced cleavage (S_1). Incipient crenulation cleavage (S_2) can be traced from aligned small white mica laths and opaque minerals (Fig. 3a). Microlithons consist of quartz (70%), albite (25%), detrital opaque minerals (3%), amphibole (1%), and accessory white mica, apatite and zircon (1%) (Table 2). Grain sizes of detrital quartz, white mica and albite range from 0.2 to 0.6 mm. Some detrital grains of quartz are rotated and show pressure solution effects parallel to S_1 (Fig. 3b). The size of recrystallized quartz, albite and metamorphic mica is 0.1–0.5 mm. Anastomosing cleavage domains are smooth and are composed of white mica + chlorite + opaque minerals. Transitions between microlithons and cleavage domains are discrete. Compositions of metamorphic white mica are muscovite-phengite (3.16–3.36 Si per formula unit -p.f.u.-, X_{Mg} (=Mg/(Mg + Fe)) = 0.54–0.62 and X_{Na} (=Na/(Na + K + Ba)) = 0.02–0.04; Table 3). X_{Mg} in chlorite is 0.33–0.36 with 5.40–5.71 Si p.f.u.

Sample 09A20 is a fine-grained metagreywacke with granoblastic texture and a slightly folded spaced cleavage (S_1). Microlithons consist of quartz (75%), albite (21%), white mica (3%) and zircon and apatite as accessory phases (1%, Table 2). Grain sizes of detrital quartz and albite are up to 0.3 mm. Sub-parallel cleavage domains are smooth and consist of white mica + chlorite + opaque minerals. Transitions between cleavage domains and microlithons are discrete. Flakes of white mica (phengite) with 3.26–3.35 Si p.f.u., a relatively constant X_{Mg} ranging from 0.49 to 0.56 and X_{Na} between 0.02 and 0.06 are present (Table 3). X_{Mg} in chlorite is 0.32–0.34 with 5.30–5.32 Si p.f.u.

Metabasalt sample QM 2–08 is a hypabysal tholeiite with subophitic textures that consists of relics of clinopyroxene (diopside and augite, Boedo, 2015) with grain size up to 2.4 mm, and minor brown amphibole, ilmenite and apatite (Fig. 3c–d). Plagioclase is replaced by albite and sericitic white mica (Fig. 3c), but one analysis yielded a relic magmatic composition of $X_{Ab} = 0.56$, $X_{An} = 0.43$, $X_{Or} = 0.01$. This igneous paragenesis is partially replaced by a low-grade metamorphic assemblage: chlorite + white mica + albite + epidote + titanite + actinolite + quartz + magnetite (Fig. 3d; Table 2). Chemical composition of white mica is: 3.20–3.44 Si p.f.u (phengite; Fig. 4) and $X_{Mg} = 0.45$–0.78 (Table 3). Chlorite is characterized by X_{Mg} of 0.51–0.53 and 5.59–5.72 Si p.f.u. Epidote has 0.33–0.56 Fe^{3+} p.f.u. and 0.003–0.007 Mn p.f.u.

Table 2
Low-grade metamorphic assemblages of metasedimentary and metabasaltic rocks. Detrital and igneous phases that are still recognizable on thin-section are also included. Abbreviations of minerals are: Ab: albite, Act: actinolite, Am: amphibole, Ap: apatite, Cal: calcite, Chl: chlorite, Cpx: clinopyroxene, Ep: epidote, Grt: garnet, Hbl: hornblende, Ilm: ilmenite, Kf: potassic feldspar, Mag: magnetite, Op: opaque minerals, Opx: orthopyroxene, Pl: plagioclase, Pu: pumpellyite, Qtz: quartz, Stlp: stilpnomelane, Ttn: titanite, Wm: white mica, Zr: zircon.

Low-grade	Metamorphic phases													Detrital phases					
Metasedimentary	Am	Grt	Pu	Ep	Chl	Wm	Kf	Ab	Qtz	Ttn	Cal	Stlp	Op	Qtz	Pl	Am	Wm	Ap	Zr
CP 26-10					x	x		x	x				x	x	x	x	x	x	x
09A20					x	x		x	x				x	x	x		x	x	x
																Igneous phases			
Metabasalt	Act	Grt	Pu	Ep	Chl	Wm	Kf	Ab	Qtz	Ttn	Cal	Stlp	Mag	Cpx	Opx	Hbl	Pl	Ilm	Ap
QM 2-08	x			x	x	x		x	x	x			x	x		x	x	x	x

Table 3
Representative chemical analyses of white mica and chlorite from metagreywackes (09A20, CP 26–10) and white mica, chlorite and actinolite from metabasalt (QM 2–08).

Sample	CP 26-10									09A20								QM 2-08											
Mineral	White mica					Chlorite				White mica						Chlorite		White mica						Chlorite				Actinolite	
SiO_2	48.32	46.43	49.13	48.90	48.06	25.46	24.74	26.35	26.33	49.80	49.33	48.37	47.53	49.54	48.65	24.03	24.07	49.80	50.85	49.29	50.83	48.10	49.71	26.33	26.35	26.21	27.12	50.86	51.68
Al_2O_3	26.74	29.75	27.65	28.40	27.35	20.15	20.69	21.27	19.97	28.75	28.29	29.24	29.31	28.44	28.13	20.34	20.49	25.84	26.04	26.98	25.82	32.70	31.39	19.10	19.12	18.97	18.99	2.72	2.88
TiO_2	0.35	0.47	0.26	0.11	0.20	0.06	0.06	0.04	0.05	0.22	0.27	0.20	0.30	0.33	0.25	0.07	0.08	0.05	0.05	0.06	0.04	0.15	0.10	0.05	0.02	0.02	0.11	0.41	0.59
FeO	3.78	2.60	3.14	2.61	3.06	31.53	32.23	30.30	32.06	3.14	3.76	3.51	3.75	3.19	3.35	33.69	33.23	2.02	3.23	2.56	2.78	2.24	1.60	25.48	26.10	26.04	25.37	11.11	13.76
Fe_2O_3	2.34	2.47	–	–	–	–	–	–	–	–	–	–	–	–	–	–	–	2.24	–	1.38	–	–	–	–	–	–	–	7.66	2.32
MgO	2.48	1.93	2.34	2.39	2.36	9.77	9.86	9.09	9.04	2.27	2.42	2.15	1.98	2.18	2.22	9.01	9.56	3.97	3.43	3.42	3.60	1.03	2.08	15.99	15.32	15.59	15.62	12.17	13.13
MnO	0.04	0.01	–	0.01	–	0.40	0.45	0.41	0.43	0.01	0.03	–	0.02	0.04	0.01	0.73	0.69	0.07	–	0.02	0.04	0.01	–	0.41	0.38	0.37	0.42	0.36	0.20
CaO	0.03	0.02	0.02	–	0.05	0.03	0.03	–	0.14	0.04	–	–	–	0.01	0.04	0.04	–	0.04	0.93	0.04	0.14	0.05	0.05	–	–	–	–	10.31	11.66
Na_2O	0.14	0.28	0.20	0.14	0.11	–	0.01	0.02	0.04	0.12	0.15	0.35	0.42	0.12	0.13	0.01	–	0.08	0.08	0.14	0.10	0.13	0.11	–	–	–	–	0.82	0.87
K_2O	10.40	9.83	9.98	9.58	9.92	0.28	0.06	0.84	0.37	10.97	10.60	10.13	10.53	10.73	10.68	0.11	0.07	10.45	10.23	10.60	10.23	9.92	10.05	–	–	–	–	0.15	0.10
BaO	0.21	0.18	0.19	0.26	0.21	0.00	–	0.08	–	0.20	0.17	0.20	0.14	0.20	0.22	–	–	–	–	–	–	–	–	–	–	–	–	–	–
H_2O	4.40	4.40	4.39	4.40	4.31	10.98	10.99	11.15	11.06	4.47	4.44	4.41	4.38	4.44	4.38	10.83	10.89	4.44	4.44	4.43	4.43	4.50	4.55	11.31	11.27	11.25	11.38	2.03	2.04
Total	99.24	98.38	97.30	96.78	95.62	98.66	99.10	99.55	99.50	99.99	99.45	98.56	98.36	99.22	98.06	98.85	99.06	99.00	99.29	98.93	98.02	98.85	99.62	98.68	98.55	98.46	99.01	98.60	99.24
Cations																													
Si	3.29	3.16	3.36	3.34	3.35	5.56	5.40	5.67	5.71	3.34	3.33	3.29	3.26	3.35	3.33	5.32	5.30	3.36	3.43	3.33	3.44	3.20	3.27	5.59	5.61	5.59	5.72	7.52	7.59
$Al^{(IV)}$	0.71	0.84	0.64	0.66	0.65	2.44	2.60	2.33	2.29	0.66	0.67	0.71	0.74	0.65	0.67	2.68	2.70	0.64	0.57	0.67	0.56	0.80	0.73	2.41	2.39	2.41	2.28	–	0.41
Ti	0.02	0.02	0.01	0.01	0.01	0.01	0.01	0.01	0.01	0.01	0.01	0.01	0.02	0.02	0.01	2.63	2.62	0.01	0.003	0.003	0.002	0.01	0.005	0.008	0.003	0.003	0.02	0.05	0.06
$Al^{(VI)}$	1.44	1.55	1.58	1.62	1.59	2.75	2.72	3.06	2.81	1.61	1.58	1.63	1.62	1.61	1.60	0.01	0.01	1.42	1.50	1.49	1.50	1.77	1.71	2.36	2.41	2.36	2.43	0.47	0.09
Fe^{3+}	0.12	0.13	–	–	–	–	–	–	–	–	–	–	–	–	–	–	–	0.11	–	0.07	–	–	–	–	–	–	–	0.85	0.26
Fe^{2+}	0.22	0.15	0.18	0.15	0.18	5.76	5.88	5.45	5.81	0.18	0.21	0.20	0.21	0.18	0.19	6.24	6.12	0.11	0.18	0.14	0.16	0.12	0.09	4.52	4.65	4.64	4.47	1.37	1.69
Mg	0.25	0.20	0.24	0.24	0.25	3.18	3.21	2.91	2.92	0.23	0.24	0.22	0.20	0.22	0.23	2.97	3.14	0.40	0.35	0.34	0.36	0.10	0.20	5.06	4.86	4.96	4.91	0.05	0.03
Mn	0.002	0.001	–	–	–	0.07	0.08	0.08	0.08	0.001	0.002	–	0.001	0.002	0.001	0.14	0.13	0.004	–	0.001	0.002	–	–	0.07	0.07	0.07	0.07	2.68	2.87
Ca	0.002	0.002	0.001	–	0.004	0.01	0.01	–	0.03	0.003	–	–	–	0.001	0.003	0.01	–	0.003	0.07	0.003	0.01	0.004	0.003	–	–	–	–	1.63	1.83
Na	0.02	0.04	0.03	0.02	0.01	0.00	0.00	0.01	0.02	0.02	0.02	0.05	0.06	0.02	0.02	0.004	–	0.01	0.01	0.02	0.01	0.02	0.01	–	–	–	–	0.24	0.25
K	0.90	0.85	0.87	0.83	0.88	0.08	0.02	0.23	0.10	0.94	0.91	0.88	0.92	0.92	0.93	0.03	0.02	0.90	0.88	0.91	0.88	0.84	0.84	–	–	–	–	0.03	0.02
Ba	0.006	0.005	0.005	0.007	0.006	–	–	0.007	–	0.005	0.009	0.005	0.004	0.005	0.006	–	–	–	–	–	–	–	–	–	–	–	–	–	–

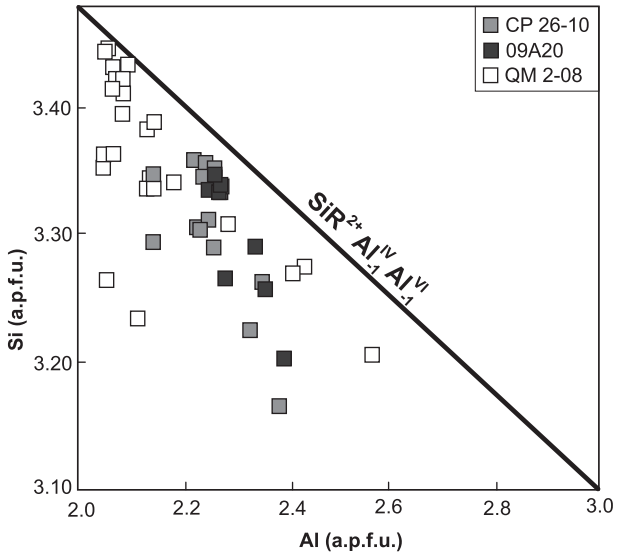

Fig. 4. Si–Al variation diagram of white mica for the studied metagreywackes and metabasalt samples.

5. Geothermobarometry

Our P-T pseudosections for the bulk-rock compositions of two metagreywacke samples CP 26–10 and 09A20 and metabasalt sample QM 2–08 result the first P-T conditions estimated for the southern low-grade metamorphic sector of the Precordillera mafic-ultramafic belt.

Stability fields for mineral assemblages calculated for sample CP 26–10 (Fig. 5) show that white mica and quartz occur throughout the whole P-T range (2–10 kbar, 200-400 °C). Chlorite is absent below 225 °C, but it is present in all assemblages formed above 340 °C, for the whole range of pressure range considered here (Fig. 5). Between 225° and 340 °C, formation of chlorite is pressure dependent. Chlorite is absent in the assemblages formed at higher pressure. Albite is present in all parageneses developed below c. 7.5 kbar Above 310 °C, albite also appears in all assemblages formed at 7.5–10 kbar.

In the calculation result of sample CP 26–10, phengite can be associated with chlorite+paragonite + lawsonite + titanite + albite + quartz (dashed field of the pseudosection Fig. 5). The observed mineral assemblage is close to this calculated paragenesis although paragonite and lawsonite were not identified. These minerals are predicted to occur in a small amounts (~0.5% vol. and between 0.8 and 2.8% vol., respectively). It could be inferred that they were not identified due to their low proportions and/or because they were decomposed along the retrograde P-T path. The P-T field of the observed assemblage (dashed field in Fig. 5) is cut by the isopleth of maximum observed Si content (3.36 p.f.u.) in white mica, at 315-395 °C and 7.6–9.3 kbar. It is possible to consider these data as the peak P-T conditions reached by this rock since the calculated paragenesis is relatively consistent with the observed mineral assemblage and no retrograde assemblages or textures were identified.

In metagreywacke sample 09A20 (Fig. 6), quartz, white mica (phengite) and rutile appear throughout the whole calculated P-T range, whereas albite does not occur below 300 °C at pressures above 8 kbar. Above approximately 325 °C, chlorite is present in all assemblages formed in the range of pressure range considered for here, whereas below c. 225 °C chlorite is absent in the calculated mineral assemblages formed in the whole range of pressure considered. The presence of chlorite is pressure dependent between 225° and 325 °C and absent in assemblages formed at higher pressure.

In the calculation result of sample 09A20, chlorite can be associated with white mica + paragonite + titanite + albite +

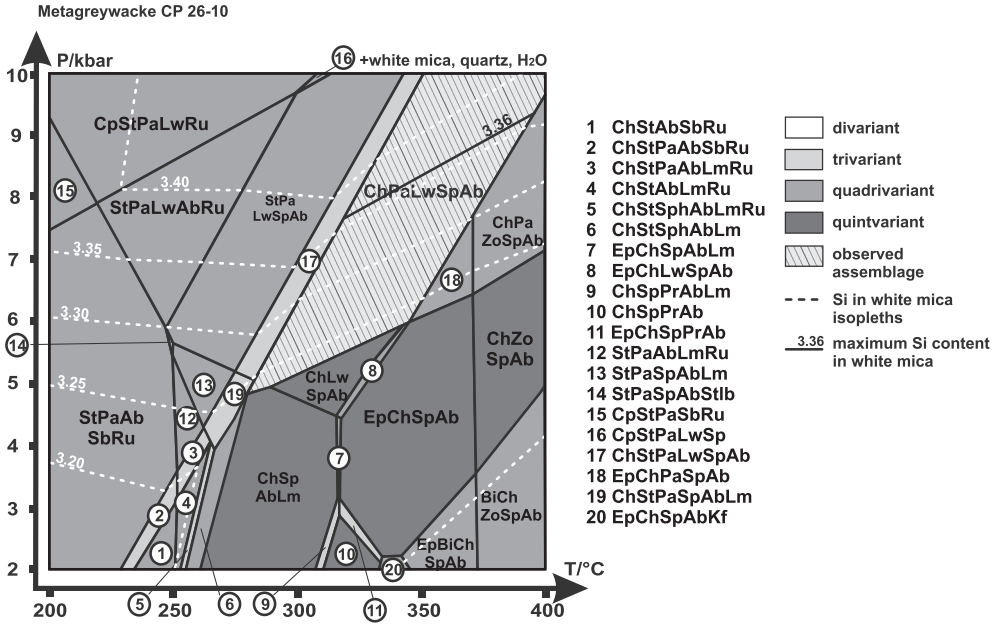

Fig. 5. P–T pseudosection for metagreywacke CP 26–10 from the Peñasco Formation calculated for the whole-rock composition in the system Na–Ca–K–Fe–Mg–Al–Si–Ti–H–O with the PERPLE_X software package (Connolly, 1990). Shading indicates the degree of variance as shown. Isopleths of Si p.f.u. in white mica are shown by white dotted lines. The highest Si content is indicated as bold solid line within the field of the observed assemblage (hatched). Abbreviations of minerals and end-member components are: Ab: albite, Am: amphibole, Bt: biotite, Ch: chlorite, Cp: clinopyroxene, Ep: epidote, Gt: garnet, Kf: potassic feldspar, Lm: laumontite, Lw: lawsonite, Pa: paragonite, Ph: phengite, Pu: pumpellyite, Qz: quartz, Ru: rutile, St: stilpnomelane, Sp: titanite, Sb: stilbite, Wm: white mica, Zo: zoisite, H_2O: aqueous fluid.

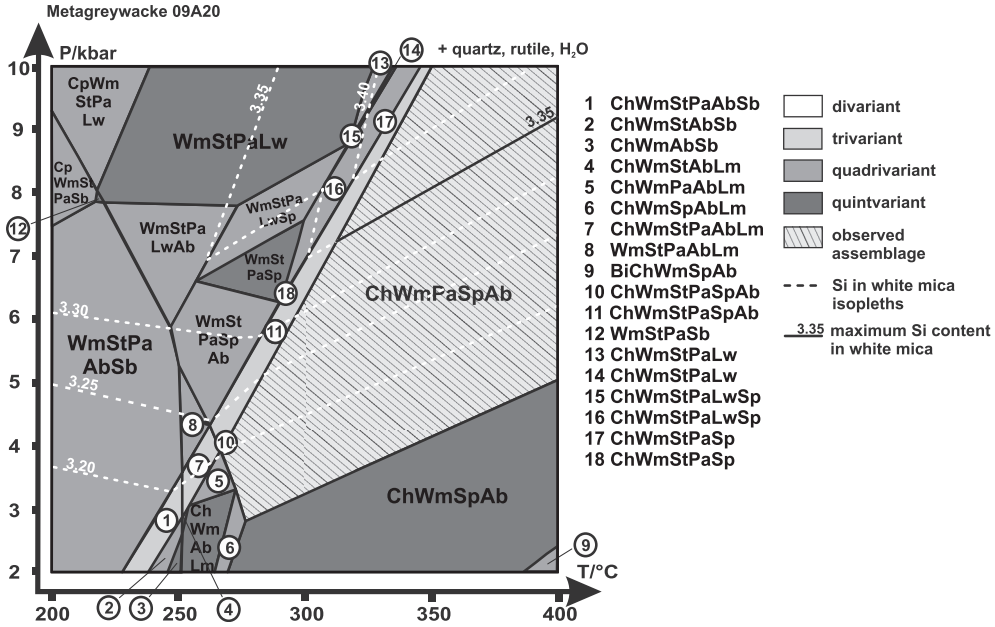

Fig. 6. P–T pseudosection for metagreywacke 09A20 from the Peñasco Formation calculated for the whole-rock composition in the system Na–Ca–K–Fe–Mg–Al–Si–Ti–H–O with the PERPLE_X software package (Connolly, 1990). For abbreviations and references see Fig. 5.

quartz + rutile (dashed field in the pseudosection of Fig. 6). The observed mineral assemblage observed in sample 09A20 is close to the calculated paragenesis, although paragonite and titanite were not identified. Both minerals are predicted to occur in small amounts (~0.5% vol. for titanite and up to 5% vol. for paragonite). It is inferred that these minerals were not recognized due to their very low proportion or because they were altered.

The P-T field of the observed assemblage is cut by the isopleth of the maximum observed Si content 3.35 p.f.u. in white mica at 310-(400°)C and 7.2–9.2 kbar. These data may be considered as the highest P-T conditions recorded by this rock as neither retrograde assemblages nor textures were identified and the calculated mineral paragenesis is relatively consistent with the recognized assemblage.

Chlorite is present in all P-T fields for mineral assemblages calculated for metabasalt QM 2–08 (Fig. 7). Above c. 280 °C, white-mica is present at pressures above c. 3 kbar. The presence of albite is P-T dependent and absent in assemblages formed at higher pressure and lower temperature.

The metamorphic conditions of metabasalt QM 2–08 can be restricted to the P-T field between the pumpellyite- and lawsonite-out and the biotite-in curves (Fig. 7), since none of these minerals was recognized in thin-section. In the calculation result for this sample, chlorite is associated with epidote + white mica + actinolite + titanite + albite + quartz. The observed mineral assemblage is close to the paragenesis marked by the dashed field of the pseudosection in Fig. 7, even though magnetite was noted that does not appear in this pseudosection. This P-T field is intersected by the isopleths of maximum Si content in white mica (3.44 p.f.u.) and maximum Na content in actinolite (0.24 p.f.u.). Resulting P-T conditions of 7.0-(9.2) kbar, 345-(400°)C are similar to those obtained for metagraywackes 09A20 and CP 26–10.

Considering an optimal overlap of the calculated P-T fields of the observed assemblages and the isopleths of the maximum Si contents of white mica in the three pseudosections, the maximum P-T conditions should be in the range of 345–395 °C and 7.0–9.3 kbar, if similar P-T conditions are assumed in the study area. These estimations are consistent with the observed assemblages in the samples which occurred in the high-pressure low-temperature region of the greenschist facies in the transitional field to the blueschist facies.

6. Discussion

The information obtained from the calculated P-T pseudosections reveals that the metasedimentary and metabasaltic rocks from the Peñasco Formation experienced high-pressure/low-grade metamorphism at 345–395 °C and 7.0–9.3 kbar (Fig. 8). Because only minor differences were observed for the estimated P-T conditions between samples of different protoliths, we assume a homogeneous metamorphic evolution for the rocks of the Peñasco Formation. The resulting geothermal gradient of 13 °C/km is somewhat higher than those derived for rocks of the suture zone between Chilenia and Cuyania (7-12°C/km; Ruviños *et al.*, 1997; Massonne and Calderón, 2008; Willner *et al.*, 2011; Martínez *et al.*, 2012). Nevertheless, it is still comparable with subduction zone geothermal gradients (3-15°C/km; Liou *et al.*, 1990; Ernst, 2001; Zhang *et al.*, 2003). The here derived P-T conditions (high-pressure greenschist facies) conditions can be attained to depths of about 25–32 km (calculated with a mean crustal density of 2.8 g/cm^3), and were related to the maximal burial depth of the sedimentary and basaltic rocks from the upper part of a downgoing slab or, alternatively, part of the base of an accretionary wedge within the collision zone between the Chilenia microcontinent and western Gondwana.

Furthermore, the temperature range estimated for rocks of the Peñasco area is also consistent with those calculated by Voldman *et al.* (2010), where the Conodont Alteration Index (CAI = 5) suggests that peak temperatures were between ~300 and 480 °C.

An Ar/Ar plateau age of 384.5 ± 0.5 Ma was related to white mica growth during peak P-T conditions in the low-grade metamorphic rocks of the Cortaderas area by Davis *et al.* (1999). We assume a similar age for the Peñasco Formation due to the presence of similar metamorphic rocks in both our study and the Cortaderas areas (Fig. 1b). If this assumption is correct, there would be a difference between the time of deposition of the protoliths of the low-grade

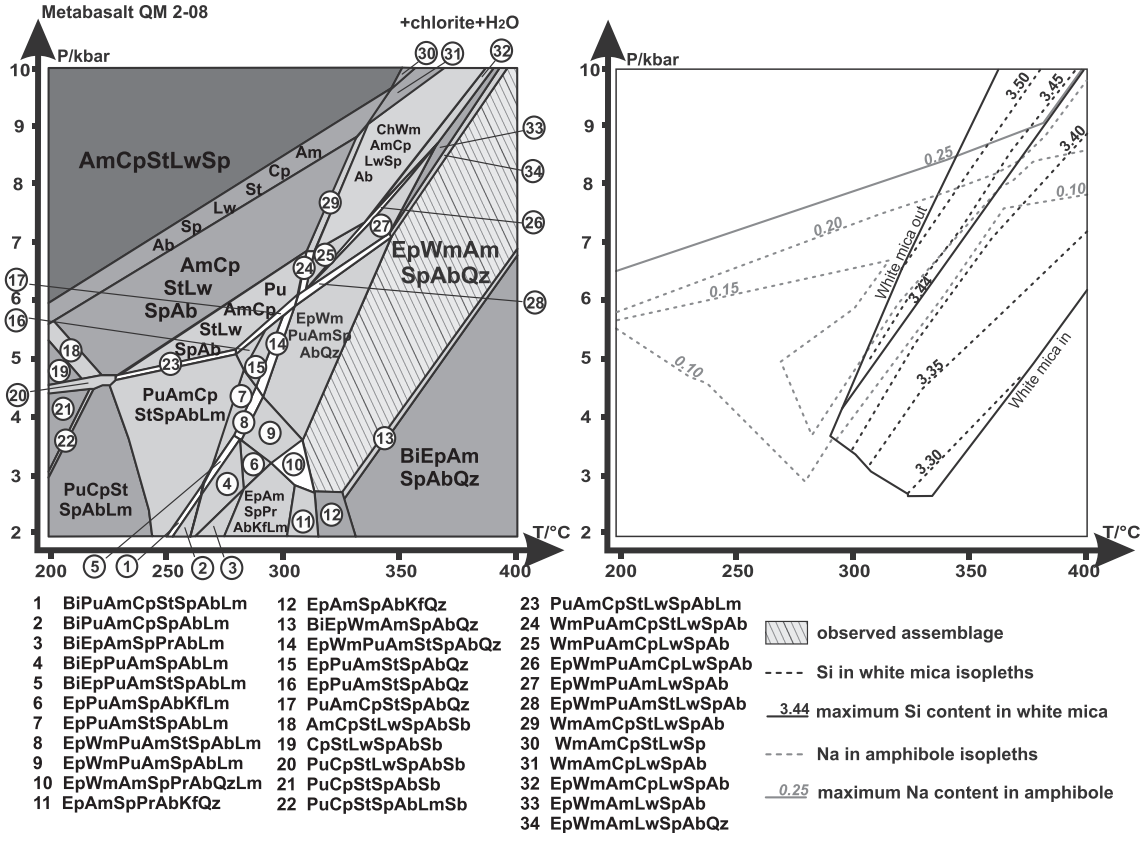

Fig. 7. P-T pseudosection for metabasalt QM 2–08 from the Peñasco Formation calculated for the whole-rock composition in the system Na-Ca-K-Fe-Mg-Al-Ti-Si-H-O with the PERPLE_X software package (Connolly, 1990). Isopleths of Si p.f.u. in white mica (black dotted line) and Na p.f.u. in actinolite (grey dotted line) are shown. Highest and lowest Si and Na contents are indicated as bold solid lines within the field of the observed assemblage (hatched). For abbreviations and references see Fig. 5.

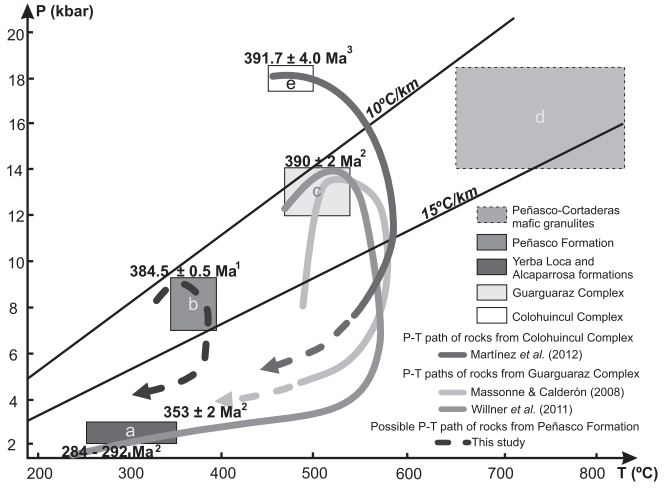

Fig. 8. P-T diagram considering the metamorphic peak conditions for the Precordillera units (Peñasco, Alcaparrosa and Yerba Loca formations) and the metamorphic P-T-paths for the Guarguaraz and Colohuincul complexes. P-T data taken from: field a- Robinson *et al.* (2005); b- This work; c- Massonne and Calderón (2008) and Willner *et al.* (2011); d- Boedo (2015); e– Martínez *et al.* (2012). Ages taken from: 1- Davis *et al.* (1999), 2- Willner *et al.* (2011) and 3- Martínez *et al.* (2012).

metasediments in the Lower Paleozoic and the Middle Devonian age of high-pressure metamorphism due to burial during continent-microcontinent collision. An alternative burial of the sediments could have been occurred by accretion within an accretionary prism prior to collision. In this case, however, deposition happened close or during the accretion event as proved, for instance, for the Late Paleozoic coastal accretionary prism of Chile (Willner *et al.*, 2005, 2008). However, more precise age data for the low-grade event are required in the future to rule out or prove this possibility.

South of the study region, in the Sierra de Guarguaraz (Frontal Cordillera), Massonne and Calderón (2008) and Willner *et al.* (2011) obtained P-T-t paths where peak metamorphic conditions (12–14 kbar, 470°-530 °C) were followed by a decompression path with a slight increase in temperature (5 kbar, 560 °C), reaching temperatures below 350–400 °C at pressures of 2–3 kbar (Fig. 8). Willner *et al.* (2011) dated the peak of high-pressure metamorphism at 390 ± 2 Ma (Eifelian; Lu-Hf mineral isochrones) and correlated this age with the collision event. This age is similar to the Ar/Ar age of 385.5 ± 0.5 Ma derived by Davis *et al.* (1999) in the Cortaderas area suggesting a similar age of collision in the low-grade areas of the collision zone. In the Guarguaraz Complex, Willner *et al.* (2011) also derived a $^{40}Ar/^{39}Ar$ plateau age of 352.7 ± 0.6 Ma of white mica and fission track ages in zircon at 284 ± 19 and 295 ± 18 Ma interpreted as cooling ages under 350 °C and 280 °C, respectively (Fig. 8). Hence, relatively low exhumation rates of 0.9–1.2 mm/a were estimated for the period 390-353 Ma and even lower exhumation rates of 0.1–0.05 mm/a for the period of 353–290 Ma.

Similarly, Massonne and Calderón (2008) and Willner *et al.* (2011) regard the P-T evolution of the Guarguaraz Complex as characteristic for crustal thickening by collision ruling out an earlier proposal of an accretionary prism (López and Gregori, 2004). The main arguments are: (1) the significantly higher burial depths of the Guarguaraz Complex compared to maximum thicknesses of

40 km known from accretionary prisms (Ring and Brandon, 1999) and (2) the heating during early decompression after the maximum pressure (Fig. 8) contrasting with typical decompression-cooling paths in accretionary prisms (e.g. Willner *et al.*, 2005, 2012). Similarly, in the northern area of the North Patagonian Andes, Martínez *et al.* (2012) yielded a similar U-Th-Pb age of 391 ± 4 Ma in monazite, which was also related to high pressure metamorphic conditions (18 kbar at 440 °C) and the collision event. The P-T-t path derived by these authors partly coincides with those of the Guarguaraz Complex (Fig. 8). The differences between these paths and the P-T conditions obtained in the study area would suggest that different portions of the collision zone are exposed within the Chilenia-western Gondwana suture.

By contrast, the estimated metamorphic gradients in metabasalts of the Rodeo and Calingasta areas (Alcaparrosa and Yerba Loca formations, Fig. 8) in the northern sector of the mafic-ultramafic belt (Fig. 1b) are higher than those of the Peñasco area. This is in accordance with the regional pattern observed in the western Argentine Precordillera, where deformation and metamorphism increase towards the west and south. Rubinstein *et al.* (1998) estimated temperatures of 239–304 °C in metabasaltic pillow lavas and dikes, and Voldman *et al.* (2010) peak temperatures of ~110°–300 °C (CAI = 2–4.5), suggesting a stacking depth of ~12 km at this latitude (calculated using 30°C/km as geothermal gradient and mentioned paleotemperatures). Robinson *et al.* (2005) derived P-T conditions of 2–3 kbar and 250-350 °C in metabasalts using Mg/Fe between actinolite and chlorite. This refers to a metamorphic gradient of 23–43°C/km and depths of 7–11 km differing from the aforementioned gradients derived from rocks which were involved in the Chilenia-western Gondwana collision zone. We postulate that the exposed northern part of the mafic-ultramafic belt was rather situated in a foreland position with respect to the collision zone. Similar metamorphic gradients of 20–25 °C/km at depths of 7–12 km were derived in similar foreland zones of continental collision zones in the Appalachians of Nova Scotia, Canada (Willner *et al.*, 2015), and the Variscides of Central Europe (Fielitz and Mansy, 1999).

The high-pressure metamorphism and related collisional processes within the collision zone of Chilenia with the composite margin of western Gondwana fits into a four-stage evolution as follows:

(1) The Guarguaraz Complex in the southernmost part of the mafic-ultramafic belt records a continental margin sedimentation in the Late Neoproterozoic as suggested by acritarchs and a Sm-Nd protolith age of 655 Ma for a metabasite (López de Azarevich *et al.*, 2009) and detrital zircon populations (Willner *et al.*, 2008). This sedimentary environment would be compatible with the existence of an ocean between the Chilenia and the Cuyania microcontinents at that time (Fig. 9a). During Early Paleozoic times, this ocean extended further north (present coordinates) as proved by conspicuous Late Neoproterozoic-Silurian continental margin sedimentation along the western margin of the Argentine Precordillera. This period of time is indicated by youngest U/Pb ages of detrital zircon populations in the San Isidro-Bonilla (603-592 Ma; Abre *et al.*, 2012; Gregori *et al.*, 2013, Fig. 1b) and the Calingast a-Rodeo (526-458 Ma; Abre *et al.*, 2012) areas and U/Pb zircon crystallization ages of E-MORB basalt intrusions in the Cortaderas (418–576 Ma; Davis *et al.*, 2000) and the Jagüé (454 Ma; Fauqué and Villar, 2003) areas.

(2) The approach of the Chilenia microcontinent toward the composite margin of western Gondwana led to the development of an eastward dipping subduction zone (Fig. 9b), as suggested by the presence of small calc-alkaline bodies of Devonian age in the San Rafael Block (401 ± 17 Ma; Cingolani *et al.*, 2003) and the Sierra del Carrizalito (Dessanti and Caminos, 1967; Tickyj *et al.*, 2009) and by

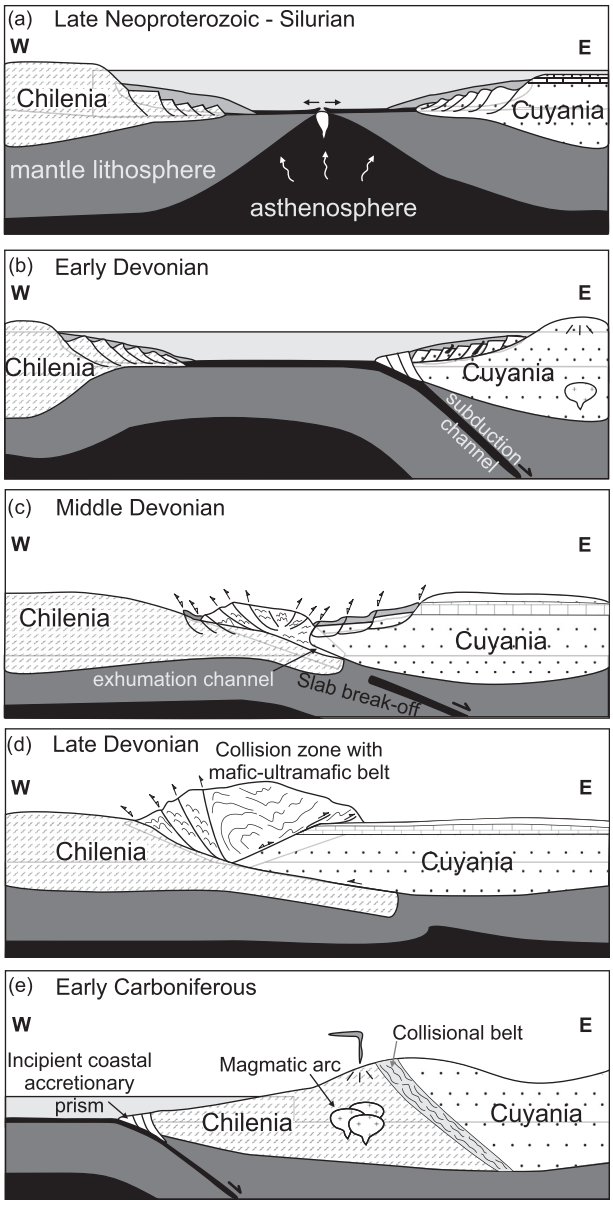

Fig. 9. Possible geodynamic scenario depicted on E–W schematic cross-sections through western South-American Gondwana from the Late Neoproterozoic to the Early Carboniferous (see text for discussion).

the overall vergence of foliations in the low-grade areas of the collision zone and in Lower Paleozoic sedimentary rocks within the Precordillera (Ramos *et al.*, 1986; von Gosen, 1997; Cortés *et al.*, 1999; Boedo, 2015). Furthermore, detrital Devonian zircon populations of magmatic origin are well detectable in Late Paleozoic sedimentary rocks in central and northern Chile (Augustsson *et al.*, 2016) giving an additional hint for the existence of a Devonian magmatic arc in the composite margin of western Gondwana.

(3) The Middle Devonian age of the final collision of Chilenia (Fig. 9c–d) is well constrained by three Lu/Hf mineral isochron ages of 390 ± 2 Ma of high-pressure metamorphic assemblages from a deeper part of the collision zone (Willner *et al.*, 2011) and by Ar/Ar phengite crystallization ages of 384.5 ± 0.5 Ma determined on rocks from a shallower part (Davis *et al.*, 2000). Slow exhumation with average rates of 0.1–0.05 mm/a occurred during the Carboniferous (Willner *et al.*, 2011). A Middle Devonian collision is also hinted by

the unconformity between deformed Devonian and overlying Carboniferous deposits (Amos and Rolleri, 1965). The oldest overlying marine sedimentary rocks are attributed to the Tournasian. Late Carboniferous marine and continental Paganzo sediments unconformably overlie all basement rocks.

(4) The collision event is followed by the formation of a new magmatic arc within Chilenia and part of the collision zone during the Early Carboniferous (Fig. 9e). This is the first arc developed at the present Pacific margin, west of the Chilenia microcontinent, resulting from subduction of oceanic crust west of Chilenia towards the east. Evidence for this arc includes ages of 348 ± 35 to 337 ± 15 Ma of granodioritic to tonalitic intrusions within the Guarguaraz Complex (Caminos *et al.*, 1979), an earliest U/Pb zircon crystallization age of 328 ± 3 Ma in the Frontal Cordillera of north-central Chile (Pineda and Calderón, 2008), a U/Pb zircon age of a leucogranite cobble of 326 ± 12 Ma with a proximal provenance within an Upper Carboniferous retrowedge basin near the coast of north-central Chile (Willner *et al.*, 2008) and a U/Pb zircon age of a granite cobble of 348 ± 2 Ma in Late Paleozoic sediments of the Calingasta area (Gallastegui *et al.*, 2014). Furthermore a pronounced detrital zircon population of magmatic origin and of Lower Carboniferous age was detected in Late Paleozoic sedimentary rocks in central and northern Chile (Augustsson *et al.*, 2016).

Apart from the initiation of an Early Carboniferous arc within Chilenia, there is firm evidence of the beginning of accretion in the Late Paleozoic coastal accretionary prism in central Chile. The prism locally contains small lenses of high-pressure rocks exhumed within a subduction channel yielding a counter-clockwise P-T path. This indicates earliest subduction against a still hot mantle wedge with metamorphic ages exceeding the prevailing Late Carboniferous metamorphic ages of the prism (Willner *et al.*, 2004). In south-central Chile at 40°57′S, the peak of high-pressure metamorphism in these rocks exhumed within a subduction channel was dated by a Lu/Hf mineral isochron at 340 ± 2 Ma (Willner *et al.*, 2009), but an earlier estimation at 361 ± 2 Ma (Ar-Ar hornblende) by Kato *et al.* (2008) also exists. Younger Ar/Ar ages in subduction channel rocks of 319 ± 1 Ma (at 34°38′S; Willner *et al.*, 2005) and 303 ± 2 Ma (at 31°32'; Willner *et al.*, 2012) indicate the end of isobaric cooling at depth in the subduction channel and hence give minimum ages of the local initiation of subduction and accretion. It seems, therefore, that the western margin of Chilenia remained a stable margin in the period ~390-350 Ma after collision.

7. Conclusions

This contribution presents the first P-T estimates for the southern low-grade metamorphic sector of the mafic-ultramafic belt (Peñasco area) of the Argentine Precordillera. Metasedimentary and metabasaltic rocks from the Peñasco Formation reached peak metamorphic conditions of 345–395 °C and 7.0–9.3 kbar that fall within the high-pressure/low-temperature region of the greenschist facies. These P-T conditions are higher than those estimated for the northern part of the belt. The conditions derived here developed under a low metamorphic gradient of 13 °C/km, which is higher than those from high-pressure, medium grade metamorphic rocks from the Guarguaraz Complex (Frontal Cordillera) and Colohuincul Complex (North Patagonian Andes) (7-12°C/km; Ruviños *et al.*, 1997; Massonne and Calderón, 2008; Willner *et al.*, 2011; Martínez *et al.*, 2012), where P-T-t paths characteristic for a continental collision zone had been derived. This reasserts that metamorphic conditions for exposed rocks in the southern sector of the belt were higher than those in the northern region. This contrast could be related to a stronger crustal thickening within the south of the collision zone between Chilenia microcontinent and the composite western Gondwana margin during the Middle Devonian, causing exhumation of sequences that were buried more deeply.

The integration and comparison of the results obtained here with those previously reported for other localities along the belt prove a long-lived sedimentation along a stable margin before the collision event. Thus, an alternative model of an accretionary prism setting for the units of the collisional belt can be discarded. This is due to a strong contrast between the long-lived sedimentation in our study area and almost contemporaneous sedimentation during accretion in an accretionary prism setting (e.g. central Chilean coastal accretionary prisms along the Pacific margin).

The metamorphic conditions constrained for the Chilenia-western Gondwana collisional belt, the presence of mafic-ultramafic bodies along this belt and the sedimentation versus deformation/metamorphism ages within the collision zone compared to the evolution of the Late Carboniferous accretionary prism developed at the Pacific margin of South America reaffirm the existence of Chilenia as a separate microcontinent.

Acknowledgements

This publication is the contribution R-195 of the Instituto de Estudios Andinos Don Pablo Groeber at UBA, Buenos Aires (Argentina). It resulted from part of FLB's PhD thesis and was financed by research projects CONICET PIP 0072 and UBACyT 20020100100862 granted to GV. The stay of FLB at Institut für Mineralogie und Kristallchemie (Universität Stuttgart) was financially supported by a short-term scholarship of the German Academic Exchange Service DAAD. Support at the microprobe by T. Theye (Stuttgart) is highly acknowledged. We are grateful to M.F. Gargiulo and E. Godoy for their very helpful critical reviews of the manuscript.

References

Abre, P., Cingolani, C.A., Cairncross, B., Chemale Jr., F., 2012. Siliciclastic ordovician to silurian units of the argentine Precordillera: constraints on provenance and tectonic setting in the proto-andean margin of Gondwana. J. S. Am. Earth Sci. 40, 1–22. http://dx.doi.org/10.1016/j.jsames.2012.07.013.

Álvarez Marrón, J., Rodriguez Fernandez, R., Heredia, N., Busquets, P., Colombo, F., Brown, D., 2006. Neogene structures overprinting Paleozoic thrust systems in the Andean Precordillera at 30°S latitude. J. Geol. Soc. 163, 949–964.

Amos, A.J., Rolleri, E.O., 1965. El Carbónico marino en el valle de Calingasta-Uspallata (San Juan-Mendoza). Bol. Inf. Pet. 368, 50–71.

Astini, R.A., Benedetto, J., Vaccari, N., 1995. The Early Paleozoic evolution of the Argentine Precordillera as a Laurentian rifted, drifted and collided terrane: a geodynamic model. Geol. Soc. Am. Bull. 17, 253–273.

Ariza, J.P., Martínez, P., Vujovich, G., Sánchez, M., Boedo, F.L., Pérez, S., 2015. Interpretación estructural de una sección geológica en las nacientes del río San Juan, a partir de datos geológicos y validación geofísica. Rev. la Asoc. Geol. Argent. 72 (4), 495–505.

Augustsson, C., Willner, A.P., Rüsing, T., Niemeyer, H., Gerdes, A., Adams, C.J., Miller, H., 2016. The crustal evolution of South America from a zircon Hf isotope perspective. Terra Nova 28, 128–137. http://dx.doi.org/10.1111/ter.12200.

Boedo, F.L., 2015. Estratigrafía de la faja máfica-ultramáfica del cordón del Peñasco, provincia de Mendoza. Ph.D. thesis. Universidad de Buenos Aires.

Boedo, F.L., Vujovich, G.I., Barredo, S.P., 2012. Caracterización de rocas ultramáficas, máficas y metasedimentarias del cordón del Peñasco, Precordillera occidental, Mendoza. Rev. la Asoc. Geol. Argent. 69 (2), 275–285.

Boedo, F.L., Vujovich, G.I., Kay, S.M., Ariza, J.P., Pérez Luján, S.B., 2013. The E-MORB like geochemical features of the Early Paleozoic mafic-ultramafic belt of the Cuyania terrane, western Argentina. J. S. Am. Earth Sci. 48, 73–84. http://dx.doi.org/10.1016/j.jsames.2013.09.003.

Buggisch, W., von Gosen, W., Henjes-Kunst, F., Krumm, S., 1994. The age of Early Paleozoic deformation and metamorphism in the Argentine Precordillera—Evidence from K-Ar data. Zentralblatt für Geologie und Palaontologie. Teil 1, 275–286.

Caminos, R., 1993. El basamento metamórfico proterozoico-paleozoico inferior. In: Ramos, V. (Ed.), Geología y Recursos Naturales de Mendoza. Relatorio 12° Congreso Geológico Argentino y 2° Congreso de Exploración de Hidrocarburos, pp. 11–19. Mendoza, Argentina.

Caminos, R., Cordani, U., Linares, E., 1979. Geología y geocronología de las rocas metamórficas y eruptivas de la Precordillera y Cordillera Frontal de Mendoza. In: 2° Congreso Geológico Chileno, pp. 43–61. Arica, Chile.

Cingolani, C.A., Basei, M., Llambias, E., Varela, R., Chemale Jr., F., Siga Jr., O., Abre, P., 2003. The Rodeo Bordalesa tonalite, San Rafael Block (Argentina): geochemical and isotopic age constraints. In: 10° Congreso Geológico Chileno, Antofagasta, Chile. Actas CD-Rom.

Connolly, J.A.D., 1990. Multivariable phase diagrams: an algorithm based on generalized thermodynamics. Am. J. Sci. 290, 666–718.

Cortés, J.M., Kay, S.M., 1994. Una dorsal oceánica como origen de las lavas almohadilladas del Grupo Ciénaga del Medio (Silúrico-Devónico) de la Precordillera de Mendoza, Argentina. In: 7° Congreso Geológico Chileno. Actas 2, Concepción, Chile, pp. 1005–1009.

Cortés, J.M., González Bonorino, G., Koukharsky, M.L., Brodtkorb, A., Pereyra, F., 1999. Hoja geológica 3369-03 yalguaraz, Mendoza (versión preliminar). Serv. Geol. Min. Argent. escala, 1:100.000.

Cucchi, R., 1971. Edades radimétricas y correlación de metamorfitas de la Precordillera, San Juan- Mendoza, Republica Argentina. Rev. la Asoc. Geol. Argent. 26, 503–515.

Davis, J., Roeske, S., McClelland, W., Snee, L., 1999. Closing an ocean between the Precordillera terrane and Chilenia: early Devonian ophiolite emplacement and deformation in the southwest Precordillera. In: Ramos, V.A., Keppie, J.D. (Eds.), Laurentia-gondwana Connections before Pangea, vol. 336. Geological Society of America Special Publication, pp. 115–138.

Davis, J., Roeske, S., McClelland, W., Kay, S.M., 2000. Mafic and ultramafic crustal fragments of the southwestern Precordillera terrane and their bearing on tectonic models of the early Paleozoic in western Argentina. Geology 28 (2), 171–174. http://dx.doi.org/10.1130/0091-7613(2000)28.

Dessanti, R.N., Caminos, R., 1967. Edades potasio-argón y posición estratigráfica de algunas rocas ígneas y metamórficas de la Precordillera, Cordillera Frontal y sierras de San Rafael, provincia de Mendoza. Rev. la Asoc. Geol. Argent. 22 (2), 135–162.

Ernst, W.G., 2001. Subduction, ultrahigh-pressure metamorphism, and regurgitation of buoyant crustal slices-implications for arcs and continental growth. Phys. Earth Planet. Interiors 127, 253–275.

Fauqué, L.E., Villar, L.M., 2003. Reinterpretación estratigráfica y petrología de la Formación Chuscho, Precordillera de La Rioja. Rev. la Asoc. Geol. Argent. 58 (2), 218–232.

Fielitz, W., Mansy, J.-L., 1999. Pre- and synorogenic burial metamorphism in the Ardennes and neighbouring areas (Rhenohercynian zone, central European Variscides). Tectonophysics 309, 227–256. http://dx.doi.org/10.1016/S0040-1951(99)00141-9.

Gallastegui, G., González-Menéndez, L., Rubio-Ordóñez, A., Cuesta, A., Gerdes, A., 2014. Origin and provenance of igneous clasts from late palaeozoic conglomerate formations (del ratón and el planchón) in the andean Precordillera of san juan, Argentina. J. Iber. Geol. 40, 261–282. http://dx.doi.org/10.5209/rev_JIGE.2014.v40.n2.45298.

Gargiulo, M.F., Bjerg, E.A., Mogessie, A., 2011. Caracterización y evolución metamórfica de las rocas ultramaficas de la Faja del rio de las Tunas, Cordillera Frontal de Mendoza. Rev. la Asoc. Geol. Argent. 68 (4), 571–593.

Gargiulo, M.F., Bjerg, E.A., Mogessie, A., 2012. Metasomatismo en ortoanfibolitas de la faja mafica-ultramafica del rio de las Tunas, Mendoza. Rev. la Asoc. Geol. Argent. 69 (2), 163–178.

Gargiulo, M.F., Bjerg, E.A., Mogessie, A., 2013. Spinel group minerals in metamorphosed ultramafic rocks from Rio de Las Tunas belt, Central Andes, Argentina. Geol. Acta 11 (2), 133–148. http://dx.doi.org/10.1344/105.000001836.

Gerbi, C., Roeske, S.M., Davis, J.S., 2002. Geology and structural history of the southwestern Precordillera margin, northern Mendoza Province, Argentina. J. S. Am. Earth Sci. 14, 821–835.

Giambiagi, L., Mescua, J., Folguera, A., Martinez, A., 2010. Estructuras y cinemática de las deformaciones preandinas del sector sur de la Precordillera, Mendoza. Rev. la Asoc. Geol. Argent. 66 (1), 5–20.

González Menéndez, L., Gallastegui, G., Cuesta, A., Heredia, N., Rubio-Ordonez, A., 2013. Petrogenesis of Early Paleozoic basalts and gabbros in the western Cuyania terrane: constraints on the tectonic setting of the southwestern Gondwana margin (Sierra del Tigre, Andean Argentine Precordillera). Gondwana Res. 24 (1), 359–376. http://dx.doi.org/10.1016/j.gr.2012.06.016.

Gregori, D.A., Bjerg, E.A., 1997. New evidence on the nature of the Frontal Cordillera ophiolitic belt- Argentina. J. S. Am. Earth Sci. 10 (2), 147–155.

Gregori, D.A., Martinez, J.C., Benedini, L., 2013. The gondwana-south America iapetus margin evolution as recorded by lower paleozoic units of western Precordillera, Argentina: the Bonilla complex, uspallata. Ser. Correlación Geol. 29 (1), 21–80.

Haller, M.J., Ramos, V.A., 1984. Las ofiolitas famitinianas (Eopaleozoico) de las provincias de San Juan y Mendoza. In: 9° Congreso Geológico Argentino. Actas 3, Bariloche, Argentina, pp. 66–83.

Harrington, H.J., 1971. Hoja 22c "Ramblón", provincias de Mendoza y San Juan. Dirección Nacional de Geología y Minería, Boletín 114 escala 1:250.000.

Holland, T.J.B., Powell, R., 1996. Thermodynamics of order-disorder in minerals. 2. Symmetric formalism applied to solid solutions. Am. Mineralogist 81, 1425–1437.

Holland, T.J.B., Powell, R., 1998. An internally consistent thermodynamic data set for phases of petrological interest. J. Metamorph. Geol. 16, 309–343.

Holland, T.J.B., Powell, R., 2003. Activity-composition relations for phases in petrological calculations: an asymmetric multicomponent formulation. Contributions Mineralogy Petrology 145, 492–501.

Kato, T.T., Sharp, W.D., Godoy, E., 2008. Inception of a Devonian subduction zone along the southwestern Gondwana margin; ^{40}Ar-^{39}Ar dating of eclogite-amphibolite assemblages in blueschist boulders from the Coastal Range of Chile (21°S). Can. J. Earth Sci. 45, 337–351.

Kay, S.M., Ramos, V.A., Kay, R., 1984. Elementos mayoritarios y trazas de las vulcanitas ordovícicas de la Precordillera occidental; basaltos de rift oceánico temprano(?) próximo al margen continental. In: 9° Congreso Geológico Argentino. Actas 2, Bariloche, Argentina, pp. 48–65.

Liou, J.G., Maruyama, S., Wang, X., Graham, S., 1990. Precambrian blueschist terranes of the world. Tectonophysics 181, 97–111.

López, V.L., 2005. Geología y Petrología de la Cuchilla de Guarguaraz, Cordillera Frontal de Mendoza. Ph. D. Thesis. Universidad Nacional del Sur.

López, V.L., Gregori, D.A., 2004. Provenance and evolution of the Guarguaraz complex, Cordillera frontal, Argentina. Gondwana Res. 7, 1197–1208.

López de Azarevich, V.L., Escayola, M., Azarevich, M.B., Pimentel, M.M., Tassinari, C., 2009. The Guarguaraz Complex and the Neoproterozoic-Cambrian evolution of southwestern Gondwana: geochemical signatures and geochronological constraints. J. S. Am. Earth Sci. 28, 333–344. http://dx.doi.org/10.1016/j.jsames.2009.04.013.

Martínez, J.M., Dristas, J., Massonne, H.-J., 2012. Palaeozoic accretion of the microcontinent Chilenia, North Patagonian Andes: high-pressure metamorphism and subsequent thermal relaxation. Int. Geol. Rev. 54 (4), 472–490. http://dx.doi.org/10.1080/00206814.2011.569411.

Massonne, H.-J., Calderón, H., 2008. P-T evolution of metapelites from the Guarguaraz Complex, Argentina: evidence for Devonian crustal thickening close to the western Gondwana margin. Rev. Geol. Chile 35 (2), 215–231.

Massonne, H.-J., Willner, A.P., 2008. Phase relations and dehydration behavior of psammopelite and mid-ocean ridge basalt at very-low-grade to low-grade metamorphic conditions. Eur. J. Mineralogy 20, 867–879. http://dx.doi.org/10.1127/0935-1221/2008/0020-1871.

Pineda, G., Calderón, M., 2008. Geología del área Monte Patria-El Maqui, región de Coquimbo. Servicio Nacional de Geología y Minería, Carta Geológica de Chile, escala, 1:100.000.

Powell, R., Holland, T., 1999. Relating formulations of the thermodynamics of mineral solid solutions: activity modeling of pyroxenes, amphiboles and micas. Am. Mineralogist 84, 1–14.

Ramos, V.A., 2009. Anatomy and global context of the Andes: main geological features and the Andean orogenic cycle. In: Kay, S.M., Ramos, V.A., Dickinson, W.R. (Eds.), Backbone of the Americas: Shallow Subduction, Plateau Uplift, and Ridge and Terrane Collision, vol. 204. Geological Society of America Memoirs, pp. 31–65. http://dx.doi.org/10.1130/2009.1204(02).

Ramos, V.A., Jordan, T.E., Allmendinger, R.W., Mpodozis, C., Kay, S.M., Cortes, J.M., Palma, M., 1986. Paleozoic terranes of the central argentine-chilean Andes. Tectonics 5, 855–880.

Ring, U., Brandon, M.T., 1999. Ductile deformation and mass loss in the Franciscan subduction complex: implications for exhumation processes in accretionary wedges. In: Ring, U., Brandon, M.T., Lister, G.S., Willett, S.D. (Eds.), Exhumation Processes: Normal Faulting, Ductile Flow and Erosion, vol. 154. Geological Society of London Special Publication, pp. 55–86. http://dx.doi.org/10.1144/GSL.SP.1999.154.01.03.

Robinson, D., Bevins, R.E., Rubinstein, N., 2005. Subgreenschist facies metamorphism of metabasites from the Precordillera terrane of western Argentina; constraints on the later stages of accretion onto Gondwana. Eur. J. Mineralogy 17, 441–452. http://dx.doi.org/10.2747/0020-6814.47.2.177.

Rubinstein, N., Bevins, R., Robinson, D., Morello, O., 1998. Very low metamorphism in the Alcaparrosa formation, western Precordillera, Argentina. In: 10° Congreso Latinoamericano de Geología and 6° Congreso Nacional de Geología Económica. Actas 2, Buenos Aires, Argentina, pp. 326–329.

Rubinstein, N., Bevins, R.E., Robinson, D., 2000. Low grade metamorphism in the Argentine Precordillera: a record of extension at the margin of Gondwanaland?. In: 9° Congreso Geológico Chileno. Actas 2, Puerto Varas, Chile, pp. 524–527.

Ruviños, M.A., Gregori, D.A., Bjerg, E.A., 1997. Condiciones de P y T del basamento metamórfico de la Cordillera Frontal de Mendoza, Argentina. In: 8° Congreso Geológico Chileno. Actas 2, Antofagasta, Chile, pp. 1512–1516.

Tickyj, H., Rodríguez Raising, M., Cingolani, C.A., Alfaro, M., Uriz, N., 2009. Graptolitos ordovícicos en el sur de la Cordillera Frontal de Mendoza. Rev. Asoc. Geol. Argent. 64 (2), 295–302.

Thomas, W.A., Astini, R.A., 2003. Ordovician accretion of the argentine Precordillera terrane to Gondwana: a review. J. S. Am. Earth Sci. 16, 67–79. http://dx.doi.org/10.1016/S0895-9811(03)00019-1.

Villar, L.M., 1969. El complejo ultrabásico de Novillo Muerto, Cordillera Frontal, Provincia de Mendoza, Republica Argentina. Rev. la Asoc. Geol. Argent. 24, 223–238.

Villar, L.M., 1970. Petrogénesis del complejo ultrabásico de Novillo Muerto, Cordillera Frontal, Mendoza, Argentina. Rev. Asoc. Geol. Argent. 25, 87–99.

Voldman, G.G., Albanesi, G.L., Ramos, V.A., 2010. Conodont geothermometry of the lower paleozoic from the Precordillera (Cuyania terrane), northwestern Argentina. J. S. Am. Sci. 29 (2), 278–288. http://dx.doi.org/10.1016/j.jsames.2009.08.003.

von Gosen, W., 1997. Early paleozoic and andean structural evolution in the rio jachal section of the argentine Precordillera. J. S. Am. Earth Sci. 10, 361–388.

Willner, A.P., Glodny, J., Gerya, T.V., Godoy, E., Massonne, H.-J., 2004. A counterclockwise PTt-path in high pressure-low temperature rocks from the Coastal Cordillera accretionary complex of South Central Chile: constraints for the earliest stage of subduction mass flow. Lithos 73, 283–310. http://dx.doi.org/10.1093/petrology/egi036.

Willner, A.P., Thomson, S.N., Kröner, A., Wartho, J.A., Wijbrans, J., Hervé, F., 2005. Time markers for the evolution and exhumation history of a late Palaeozoic paired metamorphic belt in central Chile (34°-35°30′S). J. Petrology 46, 1835–1858.

Willner, A.P., Gerdes, A., Massonne, H.-J., 2008. History of crustal growth and recycling at the Pacific convergent margin of South America at latitudes 29°-36°S revealed by a UPb and Lu-Hf isotope study of detrital zircon from late Paleozoic accretionary systems. Chem. Geol. 253, 114–129. http://dx.doi.org/10.1016/j.chemgeo.2008.04.016.

Willner, A.P., Massonne, H.-J., Gerdes, A., Hervé, F., Sudo, M., Thomson, S., 2009. The contrasting evolution of collisional and coastal accretionary systems between the latitudes 30°S and 35°S: evidence for the existence of a Chilenia microplate. In: 12° Congreso Geológico Chileno S9 099. Santiago de Chile, Chile, 223.

Willner, A.P., Gerdes, A., Massonne, H.-J., Schmidt, A., Sudo, M., Thomson, S.N., Vujovich, G., 2011. The geodynamics of collision of a microplate (Chilenia) in Devonian times deduced by the pressure-temperature-time evolution within part of a collisional belt (Guarguaraz Complex, W-Argentina). Contributions Mineralogy Petrology 162, 303–327. http://dx.doi.org/10.1007/s00410-010-0598-8.

Willner, A.P., Massonne, H.-J., Ring, U., Sudo, M., Thomson, S., 2012. P-T evolution and timing of a late Palaeozoic fore-arc system and its heterogeneous Mesozoic overprint in north-central Chile (latitudes 31-32°S). Geol. Mag. 149, 177–207. http://dx.doi.org/10.1017/S0016756811000641.

Willner, A.P., Massonne, H.-J., Barr, S.M., White, C.E., 2013. Very low to low-grade metamorphic processes related to the collisional assembly of Avalonia in SE Cape Breton Island (Nova Scotia, Canada). J. Petrology 54 (9), 1849–1874 doi: 10.1093. petrology/egt033.

Willner, A.P., Barr, S.M., Glodny, J., Massonne, H.-J., Sudo, M., Thomson, S.N., Van Staal, C.R., White, C.E., 2015. Effects of fluid flow, cooling and deformation as recorded by $^{40}Ar/^{39}Ar$, Rb–Sr and zircon fission track ages in very low- to low-grade metamorphic rocks in Avalonian SE Cape Breton Island (Nova Scotia, Canada). Geol. Mag. 152 (5), 767–787. http://dx.doi.org/10.1017/S0016756814000508.

Zhang, L., Ellis, D.J., Arculus, R.J., Jiang, W., Wei, C., 2003. 'Forbidden zone' subduction of sediments to 150 km depth-the reaction of dolomite to magnesite + aragonite in the UHPM metapelites from western Tianshan, China. J. Metamorph. Geol. 21, 523–529. http://dx.doi.org/10.1046/j.1525-1314.2003.00460.x.